

# From Label Error Detection to Correction: A Modular Framework and Benchmark for Object Detection Datasets

1<sup>st</sup> Sarina Penquitt\*  
*Department of Mathematics*  
*University of Wuppertal*  
 Wuppertal, Germany  
 penquitt@uni-wuppertal.de

1<sup>st</sup> Jonathan Klees\*  
*Department of Mathematics*  
*University of Wuppertal*  
 Wuppertal, Germany  
 klees@uni-wuppertal.de

3<sup>rd</sup> Rinor Cakaj  
*Quality Match*  
 Heidelberg, Germany  
 rinor.cakaj@quality-match.com

4<sup>th</sup> Daniel Kondermann  
*Quality Match*  
 Heidelberg, Germany  
 dk@quality-match.com

5<sup>th</sup> Matthias Rottmann  
*Institute of Computer Science*  
*Osnabrück University*  
 Osnabrück, Germany  
 matthias.rottman@uos.de

6<sup>th</sup> Lars Schmarje  
*Quality Match*  
 Heidelberg, Germany  
 lars.schmarje@quality-match.com

**Abstract**—Object detection has advanced rapidly in recent years, driven by increasingly large and diverse datasets. However, label errors, defined as missing labels, incorrect classification or inaccurate localization, often compromise the quality of these datasets. This can have a significant impact on the outcomes of training and benchmark evaluations. Although several methods now exist for detecting label errors in object detection datasets, they are typically validated only on synthetic benchmarks or limited manual inspection. How to correct such errors systematically and at scale therefore remains an open problem. We introduce a semi-automated framework for label-error correction called REC✓D (Rechecked). Building on existing detectors, the framework pairs their error proposals with lightweight, crowd-sourced microtasks. These tasks enable multiple annotators to independently verify each candidate bounding box, and their responses are aggregated to estimate ambiguity and improve label quality. To demonstrate the effectiveness of REC✓D, we apply it to the class pedestrian in the KITTI dataset. Our crowdsourced review yields high-quality corrected annotations, which indicate a rate of at least 24% of missing and inaccurate annotations in original annotations. This validated set will be released as a new real-world benchmark for label error detection and correction. We show that current label error detection methods, when combined with our correction framework, can recover hundreds of errors in the time it would take a human to annotate bounding boxes from scratch. However, even the best methods still miss up to 66% of the true errors and with low quality labels introduce more errors than they find. This highlights the urgent need for further research, now enabled by our released benchmark.

## I. INTRODUCTION

Deep neural networks (DNNs) have become state-of-the-art for extracting information from large-scale visual data [1]–[6]. Training them for specialized and safety-critical domains, such as autonomous driving [1], [2], [5] or medical imaging [3], [6]–[8], requires vast amounts of high-quality anno-

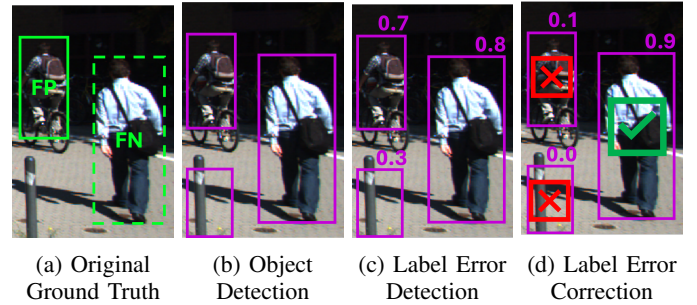


Fig. 1: Illustration of our proposed framework REC✓D. (a) Original ground truth (GT) annotations in object detection datasets often contain errors such as missing bounding boxes (false negatives, FN) or incorrect extra boxes (false positives, FP), as illustrated in the pedestrian detection example. REC✓D operates in three stages to refine the original GT: (b) Bounding box proposals are generated using pretrained object detectors. (c) These boxes are scored by a label error detection algorithm, assigning a probability (shown as a small number above each box) that the box corresponds to a labeling error. (d) Human microtasks are used to validate each box, producing an updated soft label (revised probability above box) that reflects the likelihood of the object being a true pedestrian. Boxes are then accepted or rejected based on this probability.

tated data [9]–[12]. Crowdsourcing offers a cost- and time-effective solution for building large-scale vision datasets [13] and enables scalable annotation [14]–[16], particularly when tasks are broken down into simple, quick interactions known as *microtasks* [13], [14]. The quality of labels is critical because label errors such as missing labels, incorrect classes,

\* Equal contribution.

or poor localization degrade model performance, generalization capability [17]–[24] and benchmark validity [17], [25]. Although recent research has proposed automated methods for detecting such errors in image classification [25]–[27], semantic segmentation [28], and object detection [29], few works have focused on correcting them [26], [30]–[32] and no use error detection method to reduce the reannotation costs.

We propose REC/D (see Figure 1), a semi-automated framework that transitions from label error detection to correction for object detection datasets. REC/D combines automated label error proposals from existing methods [33]–[35] with lightweight validation via microtasks. Aggregated responses capture both label correctness and ambiguity, enabling scalable and cost-effective correction. We apply REC/D to the pedestrian class in the KITTI dataset [36]. Pedestrians in KITTI represent a high-ambiguity, high-error-rate class that is both practically important (*e.g.* in autonomous driving) and methodologically challenging due to size variation, occlusion, and scene clutter [37]. Our annotations reveal at least 24.6% of previously unlabeled or incorrectly located pedestrian labels. These corrected annotations will be made publicly available as a new benchmark for evaluating methods for detecting and correcting label errors. Our analysis shows that current detection methods can be rechecked faster than humans can draw the bounding boxes for labeling. However, up to 66% of errors remain undetected, highlighting the need for improved detection strategies, which are now supported by our benchmark.

Our main contributions can be summarized as follows:

- We propose REC/D a scalable, cost-efficient framework that utilizes state-of-the-art label error detection methods, extending them to label error correction in object detection datasets which can find hundreds of errors faster than humans can annotate the bounding boxes.
- We introduce ambiguity-aware labeling through soft labels yielding high quality object labels. We demonstrate that lower quality data might introduce more errors than it is fixing. We release corrected pedestrian annotations for KITTI, enabling evaluation of label error detection methods on real-world label noise.
- With our framework we detected at least 24.6% of missing and inaccurate pedestrian annotations. However, we also find up to 66% of the errors can currently not be found by error correction methods, highlighting the importance of this research now enabled by our released benchmark.

We make our source code publicly available at <https://github.com/JonathanKlees/rechecked>.

## II. RELATED WORK

### A. Identifying Label Errors in Object Detection Datasets.

In recent years, there has been a research focus on label error detection in object detection. Cleanlab’s tool ObjectLab [35] assesses the quality of labels in object detection datasets by comparing predicted bounding boxes with ground

truth, and provides a score describing the quality of the labels. Another method, based on the instance-wise object detection loss [34], uses a two-stage object detector to detect real label errors by monitoring the regression and classification losses and using the discrepancy between predictions and ground truth labels. MetaDetect [33] is a method that performs meta classification and meta regression for predictions. Potential label errors are those predicted boxes that are evaluated as false positive ( $IoU < 0.5$  with ground truth), but the meta classifier estimates a high probability of being correct. The method LidarMetaDetect [38], [39] is a further development of MetaDetect, as it detects label errors in 3D object detection datasets. Bär *et al.* [40] developed a label refinement network that improves noisy localization labels. While we build on this recent research we go one step further and aim at correcting these labels instead of just detecting them.

### B. Label Error Correction.

In addition to detecting label errors, correcting them has also become an important step in improving label quality. Bernhardt *et al.* [41] developed an active label cleaning framework to prioritize samples for reannotation by comparing estimated label correctness and label difficulty. CROWDLAB [42] is another tool of Cleanlab that classifies crowdsourced labels for refinement to identify which samples require re-annotation. In the work of Ma *et al.* [31], annotators was formed to re-annotate the COCO [43] and Google Open Images [44] datasets to compare model performance on original and re-annotated data. Kim *et al.* [32] combines foundation models with label corrections provided by human annotators to publish PASCAL+, an updated version of the Pascal VOC dataset for semantic segmentation and Yun *et al.* [45] applied their re-labeling strategy, *ReLabel*, to re-annotate the ImageNet training set and published a corrected version. Our work focuses on the process of label error correction based on error detection, with the aim of reducing annotation costs.

### C. Ambiguity and Soft Labels in Computer Vision Datasets.

In common computer vision benchmark datasets, images or objects are usually associated with a single hard class label. However, recent research shows that this concept is not representative of the ambiguity in real data [23], [46]–[54] and even harms model performance [20]–[24], [55]. In contrast to this, soft or probabilistic labels [56] indicate a probability distribution across several classes reflecting that the correct label for an instance is not always straightforward and multiple annotators may disagree on the label. Soft labels in object detection datasets are rare but there exist methods that simulate soft labels based on single-class annotations through deep learning [57]–[59]. We extend this research by showing that the label quality is essential for correcting labels and poor quality data might even introduce more errors than it corrects. Furthermore, we release these soft labels as benchmark for future error detection and correction research.



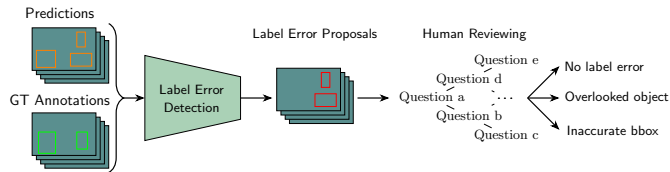


Fig. 2: Overview of our suggested workflow REC/D to detect and correct label errors in object detection datasets.

### III. METHOD REC/D

The most challenging task in label error detection is detecting missing labels, *i.e.*, objects present in the image that are missing in the ground truth (GT) annotations. Unlike inaccurate bounding box localizations and incorrect class labels, which only require verifying existing annotations and are therefore easier to identify, detecting missing labels requires a complete review of each image. We propose a semi-automatic framework that combines label error detection methods with a microtask based review process to efficiently correct label errors. It consists of three main stages: object detection, label error proposal, and microtask based correction. We provide an overview of the pipeline in Figure 2 and explain the interaction between automated and human components to detect missing labels and bounding box annotations with an inaccurate localization.

#### A. Object Detection Models

In the initial phase of the proposed framework, a trained object detector is used to obtain predictions on the respective dataset establishing the foundation of our framework. We use YOLOX [60], a one-stage detector, and Cascade R-CNN [61], a two-stage detector. YOLOX is an anchor-free detector with a decoupled head and applies stronger data augmentations, such as Mosaic or MixUp, to enhance the network’s performance. The Cascade R-CNN comprises of a sequence of detectors in its multi-stage architecture. These detectors are trained sequentially, with the output of one detector serving as the training set for the subsequent one. This particular architecture is motivated by the objective of mitigating both overfitting and quality mismatch during inference.

#### B. Label Error Detection Methods

The second stage of our framework automatically generates proposals for label errors, which are then to be reviewed manually in the third stage. These proposals are generated by integrating existing label error detection methods, including MetaDetect [33], loss-based instance-wise scoring [34] and ObjectLab [35]. Each method predicts a score that reflects the likelihood of a predicted box indicating a label error for every detected bounding box. The considered methods rely on the predictions of an object detector, which are compared to the ground truth annotations to identify overlooked objects or misfitting bounding boxes.

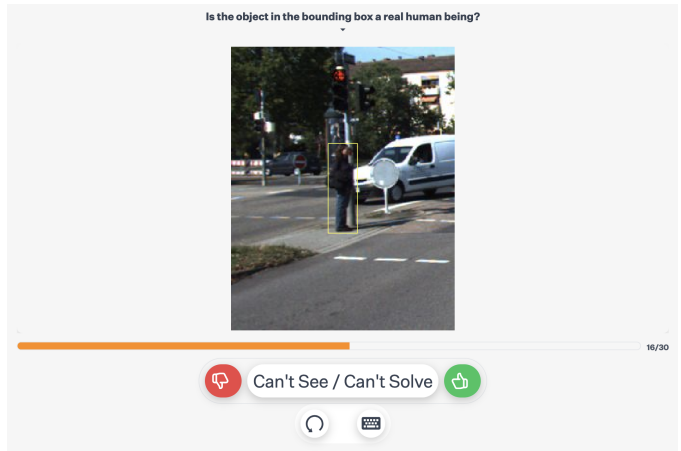


Fig. 3: Microtask interface for verifying whether the object in the bounding box is a real human being. The interface shows only the relevant region and minimal surrounding context. A clear highlight guides the annotator’s attention, and no unnecessary elements are shown that could distract from the decision.

#### C. Error Correction

From the previous stage, we obtain a collection of label error proposals that need to be manually evaluated. We created short and easy-to-answer questions consisting of a single visual task, *e.g.* whether the highlighted object is a human or not as illustrated in Figure 3. These kinds of micro-questions are also referred to as microtasks [62]. With microtasks, annotators can quickly answer one simple question at a time. We repeat the task with several people at the same time resulting in an estimate of the underlying distribution of the outcomes associated to this question.

More complex questions, such as ‘What is a pedestrian?’, are broken down into multiple microtasks, such as ‘Is it a human?’ and ‘What is the person doing?’. See subsection IV-B for the microtasks used to construct the validated annotations of the KITTI dataset. We can use the calculated soft label probability to determine whether a proposed label error is indeed erroneous or not.

### IV. EXPERIMENTAL SETUP

In the following, we describe the dataset used in our study, the object detectors evaluated, the design of our microtasks, and the metrics employed for evaluation.

#### A. Dataset Construction

We applied our label error detection and correction framework to the KITTI [36] 2D object detection dataset. We focus on the pedestrian class in KITTI as a challenging and safety-relevant use case. We consider a single class and dataset to enable a thorough investigation of the label error correction process, ensuring high-quality validation and detailed analysis, while the overall design of our framework remains dataset- and class-agnostic to support future generalization. The dataset

contains 7,481 training images and 7,518 test images showing street scenes. Since no ground truth annotations are provided for the test set, we restricted our analysis to the annotated training data. The training images include annotations for the following object classes: car, van, truck, pedestrian, person (sitting), cyclist, tram and misc. In addition, some regions are labeled as "don't care" to mark areas with unlabeled objects, reducing the likelihood of false positives during evaluation.

For our case, we randomly split the annotated training set into training (80%) and validation (20%) subsets. To ensure representative coverage, we repeated the sampling process until approximately 80% of all ground truth pedestrian annotations were assigned to the training set and 20% to the validation set. The resulting dataset consists of 5,984 training images with 3,591 pedestrian objects and 1,497 validation images with 896 pedestrians. The object detectors were trained on all annotated classes, while evaluation was limited to the class *pedestrian* on the validation set. To infer predictions for all regions of an image, we did not consider *don't care* regions during training and inference to not restrict the object detection task.

### B. Validated Ground Truth Generation

To establish a reliable evaluation benchmark, we constructed a high-quality *validated ground truth* (VGT) that achieves a very high recall by capturing every visible pedestrian. Each bounding box is associated with a probability score that reflects the likelihood of containing a pedestrian, rather than relying on a single hard label that may be erroneous. We use a two-stage microtask pipeline. In the first stage, we localize pedestrian instances. In the second stage, we validate the semantic content of each bounding box, generating soft labels that reflect annotator's uncertainty.

TABLE I: Bounding box annotation strategies. The number of aggregations refers to how many annotator-provided boxes were combined into the final box. The combined strategy merges results from both methods. Costs are reported as average per box in seconds. † Cost for keypoint annotation alone is 11.12 s. ‡ Manual effort for removal of duplicate boxes is not included.

	# Bounding Boxes	# Aggregations	Costs [s]
Direct box	2833	1.0	44.11
Keypoint-to-box	2099	3.0	92.671†
Combined box	3078	2.4	103.79‡

a) *Stage 1: Bounding box collection.*: Firstly, our aim was to identify all possible human instances in the data. To achieve this, we used two complementary task configurations, each with three annotators.

- **Direct box annotation (Microtask 1):** Multiple annotators draw tight bounding boxes around all the real humans that have not yet been marked in the image.
- **Keypoint-to-box annotation (Microtasks 2 & 3):** Multiple annotators first place keypoints on unmarked humans,

then draw a bounding box around each group of keypoints. The drawn bounding boxes are then aggregated.

Running both strategies in separate task configurations allows us to compare annotation effort and resulting recall. For constructing the VGT, we combined both methods to ensure maximal coverage of pedestrian instances. We manually removed duplicate boxes resulting from the different strategies. Further details and visual representations of the tasks are provided in Table I and the appendix.

b) *Stage 2: Semantic validation.*: In the second stage, we determine whether each bounding box contains a pedestrian. This process also serves as the foundation for error correction, as described in subsection III-C. For this purpose, we used three microtasks, each with 11 annotators (see Appendix for visual representations):

- **Microtask 4:** Is the object a pedestrian? (*Yes, No, Can't See/Can't Solve*)
- **Microtask 5:** Is the object a real human? (*Yes, No, Can't See/Can't Solve*)
- **Microtask 6:** What is the activity? (*Walking/Running/Standing, Riding/Driving a vehicle, Sitting/Lying down, Other activity, Can't See/Can't Solve*)

TABLE II: Semantic validation strategies. Column "AR" indicates whether ambiguity refinement was applied. Confidence interval (CI) widths are based on the Wilson score interval and the delta method for 95% confidence. Costs are reported as average per bounding box in seconds. ‡ Manual effort for duplicate removal is not included.

	AR	# Annotations	CI Width	Costs [s]
Is pedestrian?		11.0 ± 0.0	0.41 ± 0.08	37.87
Is human & stand/walk?		22.0 ± 0.0	0.29 ± 0.19	57.03
Is human & stand/walk?	X	33.3 ± 11.1	0.26 ± 0.16	77.85
Validated GT	X	48.2 ± 18.2	0.24 ± 0.12	124.75‡

While microtask 4 can theoretically provide sufficient information, the combination of Microtask 5 and 6 leads to increased annotator focus and reduced ambiguity. However, this approach requires twice the number of responses, as both tasks must be completed, resulting in 22 annotations per box.

To further improve soft label quality, we incorporated two additional refinement steps. First, for boxes with high disagreement in microtasks 5 and 6, we added 11 additional annotations per task. This step, referred to as *ambiguity refinement* (AR). Second, we group duplicates of the same object from stage 1. These duplicate boxes were treated as describing the same object and aggregated accordingly. This grouping was applied exclusively to the VGT. An overview is given in Table II.

The final soft label for determining whether a bounding box contains a pedestrian is computed by multiplying the soft label from microtask 5 (real human) with the soft label from microtask 6 (standing or walking).

### C. Object Detectors

The first step in our framework is to train the YOLOX and Cascade R-CNN object detectors on the KITTI dataset. For this, we used the OpenMMLab Detection Toolbox [63]. YOLOX was trained for 80 epochs on eight classes (car, van, pedestrian, cyclist, truck, misc, tram and person sitting). We chose a learning rate of 0.01, processing the images with a resolution of (640, 640) and a batch size of eight. On the test dataset, we performed evaluations and achieved an  $AP@50$  of 77.8% for the class *pedestrian* with a score threshold of 0.3. To train Cascade R-CNN, we performed 70,000 iterations with a learning rate of 0.1. Images were batched with a batch size of six and have a resolution of (1000, 600). The trained model achieved an  $AP@50$  of 63.1% for *pedestrian* with a score threshold of 0.3. After training, we made predictions on the test dataset filtering for the class *pedestrian* and a score threshold of 0.01. After applying non-maximum-suppression (NMS) with an  $IoU$  threshold of 0.5, the remaining predictions were collected and form the basis of the label error detection methods.

### D. Label Error Detection

We use the three label error detection methods introduced above, which are based on the predictions of the object detectors YOLOX and Cascade R-CNN and generate proposals for potential errors in the pedestrian annotations. We describe the implementation details of each method for generating bounding box proposals and the number of proposals to be reviewed. We also include the baseline of proposing detected bounding boxes ranked by objectness score.

*MetaDetect.* We use the MetaDetect meta classification model, which applies gradient boosting. We use the default values for all parameters and make predictions using 5-fold cross-validation on the respective hold-out set. The  $IoU$  threshold, which determines whether predictions are considered to be false positives (FP), is set to 0.5. This threshold converts the  $IoU$  values of the predictions into binary labels that are used for training the meta classification model. For each predicted bounding box, the meta classification model predicts a probability for the prediction being correct, based on which we identify label errors. Metaclassification results are listed in the appendix.

*Instance-wise Loss Method.* This label error detection method is based on object detection loss at the instance level. It requires a two-stage object detector, which is why we only apply it to Cascade R-CNN predictions. Based on images and the corresponding ground truth annotations, this method generates label error proposal boxes with a corresponding score and class prediction. We only consider proposals with a score of at least 0.01 for the class *pedestrian*.

*ObjectLab.* The detected bounding boxes can be evaluated with respect to the overlooked score with ObjectLab for object detection. Originally, only confident predictions with a probability greater than 0.95 were considered, but to infer a score for every detected bounding box, this threshold is removed. All other parameters are set to their default values.

Additionally, we consider the poor location scores of the original ground truth annotations. As there is only a single class under consideration, the swapped class label error does not occur here. As label quality scores are normalized and lower values indicate poorer label quality, we subtract these scores from 1 and interpret the result as a probability of the corresponding label issue occurring. The detected bounding boxes, as well as the original GT boxes, are then reviewed in order of probabilities.

TABLE III: Number of identified label errors for the class *pedestrian* in the KITTI dataset depending on the probability threshold for soft label annotations and the minimal height of considered objects. Through comparison of original and validated annotations, we identify a number of label errors in the original dataset even when considering only evident errors. For the definition of label errors see subsection IV-E.

Probability threshold	$p \geq 0.5$		$p \geq 0.8$	
Object Height	Overlooked	Misfitting	Overlooked	Misfitting
<i>Considering all objects</i>				
Arbitrary	683	179	272	115
$\geq 25$ pixels	454	162	218	112
$\geq 40$ pixels	157	118	83	89
<i>Considering only objects outside of 'Don't Care' regions</i>				
Arbitrary	611	176	231	113
$\geq 25$ pixels	398	159	183	110
$\geq 40$ pixels	131	115	63	87

### E. Evaluation Metrics

*Label Errors / FN in Original GT:* We match predicted bounding boxes with the original ground truth (GT) using an  $IoU$  threshold of 0.5, and with the validated GT (VGT) using a threshold of 0.1. These thresholds serve different purposes: the 0.5 threshold is standard for checking agreement with original annotations, while the 0.1 threshold allows for approximate matching against VGT, which acts as a proxy for reannotation. A prediction is considered a label error (*i.e.*, a false negative in the original GT) if it has no match in the original GT but overlaps with the VGT. We classify errors into two types: completely missing ( $IoU = 0$ ) and misaligned boxes ( $0 < IoU < 0.5$ ) see Table III. Matching is performed greedily by descending  $IoU$ , and each VGT and GT annotation is matched at most once. We can similarly also analyze the FP in the original GT, for more details see the appendix.

*Introduced Label Errors:* To assess the risk of new errors introduced by labeling strategies, we compare their outcomes against the VGT. If a semantic validation strategy disagrees with the VGT on a bounding box's label (*e.g.* one says *pedestrian*, the other *not pedestrian*), the box is misclassified. This may cause errors (FNs or FPs) to be missed or falsely introduced.

*Costs:* Each labeling strategy incurs costs for creating bounding boxes, as reported in Table I. Label error detection methods avoid these costs by using model predictions. However, all bounding boxes, whether generated by algorithms or created by humans, must be semantically validated. We

compute the total costs using the per-box validation costs from Table II. A more detailed discussion on assigning costs per individual sample is provided in the appendix.

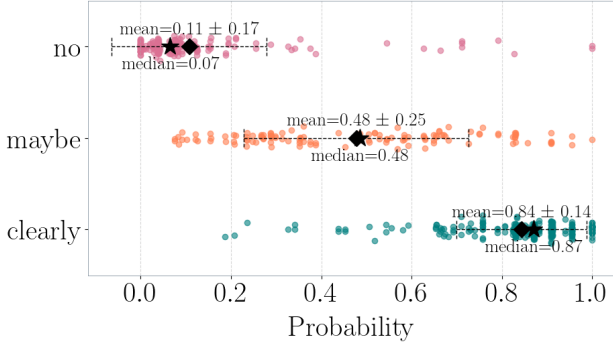
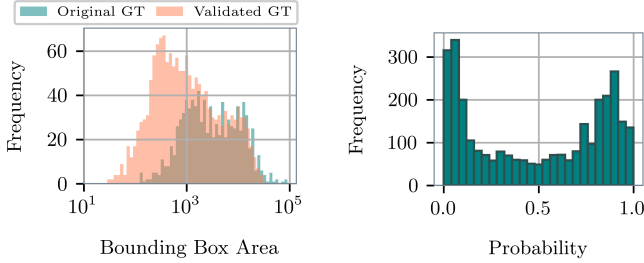


Fig. 4: Comparison of provided validated gt probability of being a human (x-axis) and human perception of being a pedestrian (y-axis). Each dot represents an annotation by three expert annotators and its corresponding probability in the VGT. The diamond represents the center of the mean, the dashed lines the standard deviation and the star the median per annotator answer.



(a) Distribution of bounding box area of original and validated annotations. Here, we consider VGT annotations with a soft label probability of 0.5 or higher. (b) Distribution of VGT soft labels. Through aggregation of multiple responses from annotators a probability for a bounding box containing a pedestrian was inferred.

Fig. 5: Details on VGT annotations including the distribution of bounding box area compared to original annotations and soft labels. We observe that VGT annotations additionally contain many small objects and the soft labels reveal that some ambiguous annotations exist while annotator agreement is usually high.

## V. NUMERICAL RESULTS

We present quantitative results for comparing the original GT with VGT, identified label errors, performance of label error detection methods with a focus on annotation costs as well as trade-offs for labeling strategies with regard to costs and quality of data.

### A. Comparison of Original and Validated Annotations

Before comparing the VGT to the original ground truth, we first verify its quality. We evaluate three aspects: whether pedestrians were missed, whether duplicate bounding boxes exist, and how well the soft labels align with human perception. In a random sample of 200 images, we found that about 0.5% of pedestrians might have been missed, and about 0.8% of pedestrian bounding boxes were duplicates. See the appendix for the full analysis and visual examples. To evaluate the alignment of soft labels with human perception, we randomly sampled 200 bounding boxes from the VGT and let three expert annotators rate them. Each annotator could choose between the labels 'clearly', 'maybe', or 'no' to indicate whether the bounding box contains a pedestrian. In Figure 4, these labels are compared with the corresponding soft label probability. The comparison shows that the categories match well with the expected scores. The category 'maybe' has a mean and median of 0.48, which is almost perfectly calibrated, as we would expect a value around 0.5. For the category 'clearly', we would expect a value around 0.8, which is consistent with the results. We conclude that the validated ground truth contains almost no missing pedestrians (about 0.5%), almost no duplicate bounding boxes (about 0.8%), and is well aligned with human perception.

We compare the validated annotations with the original annotations to determine the number of overlooked pedestrians and the number of misfitting or inaccurate bounding boxes. Overlooked pedestrians are VGT annotations that have an *IoU* of zero with any original annotation. Misfitting boxes are VGT annotations for which there is an intersecting bounding box in the original ground truth, but with an *IoU* below 0.5. We distinguish between large and small objects based on the minimum bounding box height, using thresholds of 25 or 40 pixels which relate to the difficulty levels defined in the KITTI benchmark. Additionally, we consider two different probability thresholds, 0.5 and 0.8, for the soft labels in the VGT. The distribution of soft label probabilities is shown in Figure 5b and illustrates that while most annotations show high agreement among annotators, some ambiguous cases occur. It is important to note that, unlike the original annotation protocol, the procedure described in subsection IV-B includes all pedestrians, regardless of their size or whether they fall into defined *don't care* regions. As a result, we observe that the VGT also contains small objects that were not annotated in the original data, as shown in Figure 5a.

To ensure a fair comparison, we define a default configuration for the annotations under consideration. We include all objects that have an *IoU* below 0.5 with any *don't care* region and a bounding box height of at least 25 pixels. For the VGT annotations, we apply a soft label probability threshold of 0.5 to decide whether to include them. The resulting VGT contains 1,567 annotations for the class *pedestrian*, which is 671 more than in the original ground truth. Using this configuration, we identified a total of 497 label errors in the subset of 1,497 KITTI training images. Out of these, 398 pedestrians

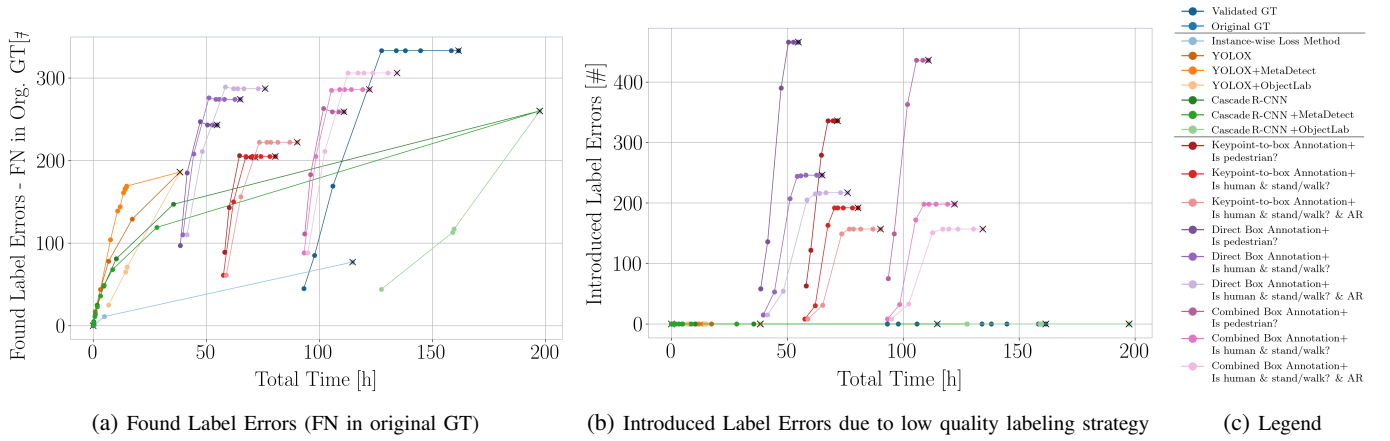


Fig. 6: Comparison of label error detection capabilities across various methods and labeling strategies, along with their respective costs. In both plots, the x-axis represents the total annotation time, while the y-axis shows the metric of interest. Each curve corresponds to a specific method, with dots marking different model confidence thresholds. The point labeled “x” indicates the lowest threshold, corresponding to the most predictions above the threshold. As the confidence threshold increases, fewer predictions are included. Methods are grouped into three categories in the legend (c): (1) ground truth baselines (original and validated), (2) automated label error detection methods, and (3) labeling strategies combining different box annotation and semantic validation techniques. The left plot (a) shows the number of detected label errors, specifically, false negatives (FNs) in the original ground truth. The center plot (b) illustrates errors introduced by different labeling strategies, demonstrating that lower-cost strategies may lead to new annotation errors. Note that automated error detection methods assume access to validated ground truth for evaluation, but also use its high cost. For a detailed description of the evaluation metrics, refer to subsection IV-E. All boxes are pre-filtered to a minimum height of 25 pixels, as per KITTI labeling guidelines. A validated ground truth label is considered a pedestrian if its soft label probability exceeds 0.8. For more relaxed filtering criteria, please see the appendix.

were missing entirely and 159 were annotated with inaccurate bounding boxes. We estimate that the original ground truth misses between 63 and 683 pedestrians, depending on the selected conditions such as minimum object size and probability threshold. This corresponds to between 7–76% relative to the 896 original pedestrian annotations. If we treat the overlooked and misaligned annotations as false negatives (FNs) relative to the original GT, we identify 293 FNs under strict conditions (applying a high confidence threshold, excluding *don’t care* regions, and enforcing size constraints) or 862 FNs when these restrictions are relaxed. This corresponds to a false negative rate (FNs / [FNs + Original GT]) ranging from 24.6% to 49%, depending on the evaluation setting. We provide visual examples of the 63 large objects that were missed, are not covered by *don’t care* regions, and have a soft label probability of 0.8 or higher in the appendix. In addition, we show random samples of other detected label errors such as inaccurate bounding box annotations and overlooked objects that either have lower confidence scores in the VGT or represent smaller pedestrians.

### B. Label Error Detection and Correction

In Figure 6a, we compare the number of false negatives (FNs) in the original ground truth (GT) detected by various label error detection methods and labeling strategies. As outlined in section III, we define label errors as FNs in the original GT. We derive two key insights from the figure: (1)

error detection methods make labeling more cost-efficient, and (2) there remains substantial room for improvement.

Among the evaluated methods, only YOLOX+MetaDetect consistently outperforms its base model. Cascade R-CNN+MetaDetect underperforms compared to Cascade R-CNN alone. ObjectLab performs significantly worse, likely due to our adaptation of its method; the original version uses a strict confidence threshold of 0.95, which we relaxed for this analysis. At such high thresholds, models provide highly confident predictions, but they cover fewer objects, limiting error discovery. For instance, using only predictions above 0.95 yields very few detected FNs, even in strong models. This highlights that restricting to high-confidence predictions alone is too limiting, even when using optimal detection techniques. Most detection-based approaches including YOLOX, Cascade R-CNN, and their error detection variants are able to find 150–200 FNs at a cost similar to or lower than the cheapest human annotation strategy. However, the base models saturate at 186 (YOLOX) and 260 (Cascade R-CNN) FNs, while the validated GT contains 333 FNs. This indicates that up to 44% of missing labels remain undetected. The gap increases under less restrictive matching conditions (*e.g.* without minimum box size), where up to 66% of FNs go unnoticed (see Appendix for full graph). This limitation stems primarily from the object detectors themselves, which constrain the set of proposed boxes. Labeling strategies show similar trends.



As summarized in Table I, strategies using keypoint-to-box annotation generate fewer boxes and thus recover fewer FNs. Additional differences can be attributed to variations in label quality across correction strategies (see subsection V-C for ablations). While detectors limit recall, our REC/D correction pipeline allows for more precise validation of the boxes they do propose and thus improving soft labeling quality. In summary, REC/D identifies hundreds of label errors in less time than it takes humans to even annotate the bounding boxes. Yet, our analysis also reveals that up to 66% of potentially recoverable FNs remain undetected, highlighting significant research opportunities for improving label error detection.

### C. Trade-offs Between Labeling Strategies and Label Quality

We evaluate the benefits and limitations of various labeling strategies in Figure 6. As expected, strategies cluster based on their bounding box annotation method discussed in the previous section. This is intuitive, since the number and quality of available boxes heavily influence the ability to identify FNs. Strategies using higher-quality soft labels consistently find more FNs. However, in less restrictive settings, *e.g.* relaxing the minimum box size (see appendix for full graph), even low-cost strategies can sometimes perform best. The second plot shows a clearer trend: the number of newly introduced errors decreases with increasing label quality. The lowest-cost semantic strategy (“Is pedestrian?”) introduces several hundred more errors than other methods. In contrast, higher-quality soft labels introduce significantly fewer mistakes. This aligns with theoretical expectations. More precise soft labels tend to have narrower confidence intervals, which reduces the probability that a sample will flip across the decision threshold due to random annotation variation. As a result, label corrections are more stable, and fewer errors are introduced. We observe even that labeling strategies introduce more new errors than they remove in the original GT for low-quality labels.

## VI. CONCLUSION

We introduced REC/D, a framework for semi-automated detection and correction of label errors in object detection datasets. For evaluation purposes, we acquired high-quality annotations based on which we identified at least 24.6% missing and inaccurate pedestrian annotations in the original KITTI dataset.

While this work demonstrated the applicability of our framework to detect and correct label errors, we also note that, under loose restrictions, up to 66% of the existing label errors were not found. This limitation stems from the distribution shift between original and validated ground truth, *i.e.*, the predictions are biased by the original ground truth which does not contain small objects in our case. One of the key motivations for releasing our soft-labeled VGT benchmark is to spur the development of better label error detection methods that overcome this recall bottleneck. We considered only a few combinations of object detectors and label error detection methods on a single dataset, focusing on the pedestrian class as an initial use case as it represents a known challenging task.

We focused on providing a detailed and focused analysis rather than giving a broad overview. Our focus is on high-quality annotations which is costly and involved plenty of manual / human effort. This cost increases with the number of data points and classes.

Our framework REC/D with its modular structure can be used with any object detector network and label error detection method. We demonstrated that it identifies hundreds of label errors faster than humans can annotate bounding boxes. We analyze different annotation procedures regarding label quality and annotation costs and show that attempting to correct datasets with poor-quality annotations may introduce more label errors than it is fixing. We announce the public release of the validated annotations for the *pedestrian* class for KITTI which includes at least 24.6% missing labels in the original GT. Furthermore, we provide an evaluation platform for the benchmark for label error detection methods for object detection labels introduced in this work.

## ACKNOWLEDGEMENTS

We thank Marius Schubert for discussion and useful advice. S.P. and M.R. acknowledge support by the German Federal Ministry of Education and Research (BMBF) within the junior research group project “UnREAL” (grant no. 01IS22069). J.K. and M.R. acknowledge support by the German Federal Ministry of Education and Research (BMBF) within the project “RELiABEL” (grant no. 01IS24019B). R.C., D.K. and L.S. also acknowledge support within the project “RELiABEL” (grant no. 01IS24019A).

## REFERENCES

- [1] S. Kuutti, R. Bowden, Y. Jin, P. Barber, and S. Fallah, “A survey of deep learning applications to autonomous vehicle control,” *IEEE Transactions on Intelligent Transportation Systems*, vol. 22, no. 2, pp. 712–733, 2020.
- [2] D. Feng, C. Haase-Schütz, L. Rosenbaum, H. Hertlein, C. Glaeser, F. Timm, W. Wiesbeck, and K. Dietmayer, “Deep multi-modal object detection and semantic segmentation for autonomous driving: Datasets, methods, and challenges,” *IEEE Transactions on Intelligent Transportation Systems*, vol. 22, no. 3, pp. 1341–1360, 2020.
- [3] A. S. Lundervold and A. Lundervold, “An overview of deep learning in medical imaging focusing on mri,” *Zeitschrift für Medizinische Physik*, vol. 29, no. 2, pp. 102–127, 2019, special Issue: Deep Learning in Medical Physics. [Online]. Available: <https://www.sciencedirect.com/science/article/pii/S0939388918301181>
- [4] L. Schmarje, M. Santarossa, S.-M. Schroder, and R. Koch, “A Survey on Semi-, Self- and Unsupervised Learning for Image Classification,” *IEEE Access*, vol. 9, pp. 82 146–82 168, 2021.
- [5] R. Hussain and S. Zeadally, “Autonomous cars: Research results, issues, and future challenges,” *IEEE Communications Surveys & Tutorials*, vol. 21, no. 2, pp. 1275–1313, 2018.
- [6] O. Oktay, J. Schlemper, L. L. Folgoc, M. Lee, M. Heinrich, K. Misawa, K. Mori, S. McDonagh, N. Y. Hammerla, B. Kainz, B. Glocker, and D. Rueckert, “Attention u-net: Learning where to look for the pancreas,” in *Medical Imaging with Deep Learning*, 2018. [Online]. Available: <https://openreview.net/forum?id=Skft7cjJM>
- [7] L. Schmarje, S. Reinhold, E. Orvoll, C.-C. Glüer, and R. Koch, “Opportunistic hip fracture risk prediction in Men from X-ray: Findings from the Osteoporosis in Men (MrOS) Study,” *Predictive Intelligence in Medicine. PRIME 2022. Lecture Notes in Computer Science*, vol. 13564, vol. MICCAI 202, pp. 103–114, 2022.
- [8] K. Kamnitsas, C. Ledig, V. F. Newcombe, J. P. Simpson, A. D. Kane, D. K. Menon, D. Rueckert, and B. Glocker, “Efficient multi-scale 3d cnn with fully connected crf for accurate brain lesion segmentation,” *Medical Image Analysis*, vol. 36, pp. 61–78, 2017. [Online]. Available: <https://www.sciencedirect.com/science/article/pii/S1361841516301839>

- [9] C. Sun, A. Shrivastava, S. Singh, and A. Gupta, "Revisiting unreasonable effectiveness of data in deep learning era," in *Proceedings of the IEEE international conference on computer vision*, 2017, pp. 843–852.
- [10] L. Schmarje, V. Grossmann, T. Michels, J. Nazarenus, M. Santarossa, C. Zelenka, and R. Koch, "Label smarter, not harder: Cleverlabel for faster annotation of ambiguous image classification with higher quality," in *German Conference of Pattern Recognition (GCPR)*, 2023, pp. 459–475.
- [11] A. Kaur, Y. Singh, N. Neeru, L. Kaur, and A. Singh, "A survey on deep learning approaches to medical images and a systematic look up into real-time object detection," *Archives of Computational Methods in Engineering*, pp. 1–41, 2021.
- [12] C. Agnew, A. Scanlan, P. Denny, E. M. Grua, P. van de Ven, and C. Eising, "Annotation quality versus quantity for object detection and instance segmentation," *IEEE Access*, vol. 12, pp. 140 958–140 977, 2024.
- [13] A. Kovashka, O. Russakovsky, L. Fei-Fei, and K. Grauman, "Crowdsourcing in computer vision," *Found. Trends. Comput. Graph. Vis.*, vol. 10, no. 3, p. 177–243, Nov. 2016.
- [14] M. Stojmenović, "Crowdsourcing applications and techniques in computer vision," in *Mobile Crowdsourcing: From Theory to Practice*, J. Wu and E. Wang, Eds. Cham: Springer International Publishing, 2023, pp. 409–431.
- [15] F. Marchesoni-Acland and G. Facciolo, "Iadet: Simplest human-in-the-loop object detection," 2023. [Online]. Available: <https://arxiv.org/abs/2307.01582>
- [16] E. Mosqueira-Rey, E. Hernández-Pereira, D. Alonso-Ríos, J. Bobes-Bascarán, and A. Fernández-Leal, "Human-in-the-loop machine learning: a state of the art," *Artif. Intell. Rev.*, vol. 56, no. 4, p. 3005–3054, Aug. 2022. [Online]. Available: <https://doi.org/10.1007/s10462-022-10246-w>
- [17] H. Song, M. Kim, D. Park, Y. Shin, and J.-G. Lee, "Learning from noisy labels with deep neural networks: A survey," *IEEE transactions on neural networks and learning systems*, vol. 34, no. 11, p. 8135–8153, November 2023. [Online]. Available: <https://doi.org/10.1109/TNNLS.2023.3152527>
- [18] O. Nahum, N. Calderon, O. Keller, I. Szpektor, and R. Reichart, "Are llms better than reported? detecting label errors and mitigating their effect on model performance," 2024. [Online]. Available: <https://arxiv.org/abs/2410.18889>
- [19] J. Jakubik, M. Vössing, M. Maskey, C. Wölflé, and G. Satzger, "Improving label error detection and elimination with uncertainty quantification," 2024. [Online]. Available: <https://arxiv.org/abs/2405.09602>
- [20] A. M. Barragán-Montero, M. Thomas, G. Defraene, S. Michiels, K. Haustermans, J. A. Lee, and E. Sterpin, "Deep learning dose prediction for IMRT of esophageal cancer: The effect of data quality and quantity on model performance," *Physica Medica*, vol. 83, pp. 52–63, 2021.
- [21] A. Saleh, I. H. Laradji, D. A. Konovalov, M. Bradley, D. Vazquez, and M. Sheaves, "A realistic fish-habitat dataset to evaluate algorithms for underwater visual analysis," *Scientific Reports*, vol. 10, no. 1, pp. 1–10, 2020.
- [22] D. Karimi, H. Dou, S. K. Warfield, and A. Gholipour, "Deep learning with noisy labels: exploring techniques and remedies in medical image analysis," *Medical Image Analysis*, vol. 65, 2020.
- [23] J. Wei, Z. Zhu, H. Cheng, T. Liu, G. Niu, and Y. Liu, "Learning with Noisy Labels Revisited: A Study Using Real-World Human Annotations," *ICLR*, pp. 1–23, 2021.
- [24] N. Tomasev, I. Bica, B. McWilliams, L. Buesing, R. Pascanu, C. Blundell, and J. Mitrovic, "Pushing the limits of self-supervised ResNets: Can we outperform supervised learning without labels on ImageNet?" *arXiv preprint arXiv:2201.05119*, 2022.
- [25] C. Northcutt, L. Jiang, and I. Chuang, "Confident learning: Estimating uncertainty in dataset labels," *Journal of Artificial Intelligence Research*, vol. 70, pp. 1373–1411, 2021.
- [26] C. G. Northcutt, A. Athalye, and J. Mueller, "Pervasive label errors in test sets destabilize machine learning benchmarks," in *Thirty-fifth Conference on Neural Information Processing Systems Datasets and Benchmarks Track (Round 1)*, 2021. [Online]. Available: <https://openreview.net/forum?id=XccDXrDNLeK>
- [27] A. Thyagarajan, E. Snorrason, C. Northcutt, and J. Mueller, "Identifying incorrect annotations in multi-label classification data," 2022. [Online]. Available: <https://arxiv.org/abs/2211.13895>
- [28] M. Rottmann and M. Reese, "Automated Detection of Label Errors in Semantic Segmentation Datasets via Deep Learning and Uncertainty Quantification," in *2023 IEEE/CVF Winter Conference on Applications of Computer Vision (WACV)*. Los Alamitos, CA, USA: IEEE Computer Society, Jan. 2023, pp. 3213–3222. [Online]. Available: <https://doi.ieeecomputersociety.org/10.1109/WACV56688.2023.00323>
- [29] Z. Hu, K. Gao, X. Zhang, J. Wang, H. Wang, and J. Han, "Probability differential-based class label noise purification for object detection in aerial images," *IEEE Geoscience and Remote Sensing Letters*, vol. 19, pp. 1–5, 2022.
- [30] Y. Jeon, K. Cho, S. Woo, and E. Kim, "A<sup>2</sup>lc: Active and automated label correction for semantic segmentation," 2025. [Online]. Available: <https://arxiv.org/abs/2506.11599>
- [31] J. Ma, Y. Ushiku, and M. Sagara, "The effect of improving annotation quality on object detection datasets: A preliminary study," in *2022 IEEE/CVF Conference on Computer Vision and Pattern Recognition Workshops (CVPRW)*, 2022, pp. 4849–4858.
- [32] H. Kim, S. Hwang, S. Kwak, and J. Ok, "Active label correction for semantic segmentation with foundation models," in *Proceedings of the 41st International Conference on Machine Learning*, ser. ICML'24. JMLR.org, 2024.
- [33] M. Schubert, K. Kahl, and M. Rottmann, "MetaDetect: Uncertainty Quantification and Prediction Quality Estimates for Object Detection," in *2021 International Joint Conference on Neural Networks (IJCNN)*, Jul. 2021, pp. 1–10.
- [34] M. Schubert, T. Riedlinger, K. Kahl, D. Kröll, S. Schoenen, S. Šegvić, and M. Rottmann, "Identifying label errors in object detection datasets by loss inspection," in *Proceedings of the IEEE/CVF Winter Conference on Applications of Computer Vision (WACV)*, January 2024, pp. 4582–4591.
- [35] U. Tkachenko, A. Thyagarajan, and J. Mueller, "Objectlab: Automated diagnosis of mislabeled images in object detection data," in *ICML Workshop on Data-centric Machine Learning Research*, 2023.
- [36] A. Geiger, P. Lenz, and R. Urtasun, "Are we ready for autonomous driving? the kitti vision benchmark suite," in *2012 IEEE Conference on Computer Vision and Pattern Recognition*, 2012, pp. 3354–3361.
- [37] V. O. Castelló, O. del Tejo Catalá, I. S. Igual, and J.-C. Perez-Cortes, "Real-time on-board pedestrian detection using generic single-stage algorithms and on-road databases," *International Journal of Advanced Robotic Systems*, vol. 17, no. 5, p. 1729881420929175, 2020.
- [38] T. Riedlinger, M. Schubert, S. Penquitt, J.-M. Kezmann, P. Colling, K. Kahl, L. Roesse-Koerner, M. Arnold, U. Zimmermann, and M. Rottmann, "Lmd: Light-weight prediction quality estimation for object detection in lidar point clouds," in *Pattern Recognition*. Cham: Springer Nature Switzerland, 2024, pp. 85–99.
- [39] —, "Lmd: Light-weight prediction quality estimation for object detection in lidar point clouds," *International Journal of Computer Vision*, vol. 133, pp. 4349–4365, 02 2025.
- [40] A. Bär, J. Uhrig, J. P. Umesh, M. Cordts, and T. Fingscheidt, "A novel benchmark for refinement of noisy localization labels in autolabeled datasets for object detection," in *2023 IEEE/CVF Conference on Computer Vision and Pattern Recognition Workshops (CVPRW)*, 2023, pp. 3851–3860.
- [41] M. Bernhardt, D. Coelho de Castro, R. Tanno, A. Schwaighofer, K. Tezcan, M. Monteiro, S. Bannur, M. Lungren, A. Nori, B. Glocker, J. Alvarez-Valle, and O. Oktay, "Active label cleaning for improved dataset quality under resource constraints," *Nature Communications*, vol. 13, 03 2022.
- [42] H. W. Goh, U. Tkachenko, and J. Mueller, "Crowdlab: Supervised learning to infer consensus labels and quality scores for data with multiple annotators," in *NeurIPS Human in the Loop Learning Workshop*, 2022.
- [43] T.-Y. Lin, M. Maire, S. Belongie, J. Hays, P. Perona, D. Ramanan, P. Dollár, and C. L. Zitnick, "Microsoft coco: Common objects in context," in *European conference on computer vision*. Springer, 2014, pp. 740–755.
- [44] A. Kuznetsova, H. Rom, N. Alldrin, J. Uijlings, I. Krasin, J. Pont-Tuset, S. Kamali, S. Popov, M. Mallocci, A. Kolesnikov, T. Duerig, and V. Ferrari, "The open images dataset v4," in *International Journal of Computer Vision*, vol. 128, no. 7, 2020, pp. 1956–1981.
- [45] S. Yun, S. J. Oh, B. Heo, D. Han, J. Choe, and S. Chun, "Re-labeling imagenet: from single to multi-labels, from global to localized labels," in *2021 IEEE/CVF Conference on Computer Vision and Pattern Recognition (CVPR)*, 2021, pp. 2340–2350.

- [46] J. Brünger, S. Dippel, R. Koch, and C. Veit, “‘Tailception’: using neural networks for assessing tail lesions on pictures of pig carcasses,” *Animal*, vol. 13, no. 5, pp. 1030–1036, 2019.
- [47] E. A. Ooms, H. M. Zonderland, M. J. C. Eijkemans, M. Kriege, B. Mahdavian Delavary, C. W. Burger, and A. C. Ansink, “Mammography: Interobserver variability in breast density assessment,” *The Breast*, vol. 16, no. 6, pp. 568–576, 2007.
- [48] T. Schoening, A. Purser, D. Langenkämper, I. Suck, J. Taylor, D. Cuvelier, L. Lins, E. Simon-Lledó, Y. Marcon, D. O. B. Jones, T. Nattkemper, K. Köser, M. Zurowietz, J. Greinert, and J. Gomes-Pereira, “Megafauna community assessment of polymetallic-nodule fields with cameras: platform and methodology comparison,” *Biogeosciences*, vol. 17, no. 12, pp. 3115–3133, 2020.
- [49] F. J. C. dos Reis, S. Lynn, H. R. Ali, D. Eccles, A. Hanby, E. Provenzano, C. Caldas, W. J. Howat, L.-A. McDuffus, B. Liu, and Others, “Crowdsourcing the general public for large scale molecular pathology studies in cancer,” *EBioMedicine*, vol. 2, no. 7, pp. 681–689, 2015.
- [50] V. Vasudevan, B. Caine, R. Gontijo-Lopes, S. Fridovich-Keil, and R. Roelofs, “When does dough become a bagel? Analyzing the remaining mistakes on ImageNet,” *Advances in Neural Information Processing Systems*, vol. 35, pp. 6720–6734, 2022.
- [51] P. Culverhouse, R. Williams, B. Reguera, V. Herry, and S. González-Gil, “Do experts make mistakes? A comparison of human and machine identification of dinoflagellates,” *Marine Ecology Progress Series*, vol. 247, pp. 17–25, 2003.
- [52] A. M. Davani, M. Díaz, and V. Prabhakaran, “Dealing with Disagreements: Looking Beyond the Majority Vote in Subjective Annotations,” *Transactions of the Association for Computational Linguistics*, vol. 10, pp. 92–110, 2022.
- [53] V. Basile, M. Fell, T. Fornaciari, D. Hovy, S. Paun, B. Plank, M. Poesio, and A. Uma, “We Need to Consider Disagreement in Evaluation,” in *Proceedings of the 1st workshop on benchmarking: past, present and future*, 2021, pp. 15–21.
- [54] L. Schmarje, M. Santarossa, S.-M. Schröder, C. Zelenka, R. Kiko, J. Stracke, N. Volkmann, and R. Koch, “A data-centric approach for improving ambiguous labels with combined semi-supervised classification and clustering,” *Proceedings of the European Conference on Computer Vision (ECCV)*, 2022.
- [55] L. Schmarje, V. Grossmann, C. Zelenka, S. Dippel, R. Kiko, M. Oszust, M. Pastell, J. Stracke, A. Valros, N. Volkmann, and R. Koch, “Is one annotation enough? A data-centric image classification benchmark for noisy and ambiguous label estimation,” *Advances in Neural Information Processing Systems*, vol. 35, pp. 33 215–33 232, 2022. [Online]. Available: [https://proceedings.neurips.cc/paper\\_files/paper/2022/file/d6c03035b8bc551f474f040fe8607cab-Paper-Datasets\\_and\\_Benchmarks.pdf](https://proceedings.neurips.cc/paper_files/paper/2022/file/d6c03035b8bc551f474f040fe8607cab-Paper-Datasets_and_Benchmarks.pdf)
- [56] P. Peng, R. C.-W. Wong, and P. S. Yu, “Learning on probabilistic labels,” in *SDM*, 2014. [Online]. Available: <https://api.semanticscholar.org/CorpusID:17158052>
- [57] Y. Li, S. Ma, X. Jiang, Y. Luan, and Z. Jiang, “Probability based dynamic soft label assignment for object detection,” *Image and Vision Computing*, vol. 150, p. 105240, 2024.
- [58] Y. Gao, Y. Zhang, Z. Huang, N. Liu, and D. Huang, “Ps-ttl: Prototype-based soft-labels and test-time learning for few-shot object detection,” in *Proceedings of the 32nd ACM International Conference on Multimedia*, ser. MM ’24. New York, NY, USA: Association for Computing Machinery, 2024, p. 8691–8700. [Online]. Available: <https://doi.org/10.1145/3664647.3681176>
- [59] C. H. Nguyen, T. C. Nguyen, T. N. Tang, and N. L. H. Phan, “Improving Object Detection by Label Assignment Distillation,” in *2022 IEEE/CVF Winter Conference on Applications of Computer Vision (WACV)*. Los Alamitos, CA, USA: IEEE Computer Society, Jan. 2022, pp. 1322–1331. [Online]. Available: <https://doi.ieeecomputersociety.org/10.1109/WACV51458.2022.00139>
- [60] Z. Ge, S. Liu, F. Wang, Z. Li, and J. Sun, “Yolox: Exceeding yolo series in 2021,” *arXiv preprint arXiv:2107.08430*, 2021.
- [61] Z. Cai and N. Vasconcelos, “Cascade r-cnn: Delving into high quality object detection,” in *Proceedings of the IEEE Conference on Computer Vision and Pattern Recognition (CVPR)*, June 2018.
- [62] B. M. Good, M. Nanis, C. Wu, and A. I. Su, “Microtask crowdsourcing for disease mention annotation in pubmed abstracts,” in *Biocomputing 2015: Proceedings of the Pacific Symposium, Kohala Coast, Hawaii, USA, January 4-8, 2015*, R. B. Altman, A. K. Dunker, L. Hunter, T. E. Klein, and M. D. Ritchie, Eds., 2015, pp. 282–293. [Online]. Available: <http://psb.stanford.edu/psb-online/proceedings/psb15/good.pdf>
- [63] K. Chen, J. Wang, J. Pang, Y. Cao, Y. Xiong, X. Li, S. Sun, W. Feng, Z. Liu, J. Xu, Z. Zhang, D. Cheng, C. Zhu, T. Cheng, Q. Zhao, B. Li, X. Lu, R. Zhu, Y. Wu, J. Dai, J. Wang, J. Shi, W. Ouyang, C. C. Loy, and D. Lin, “MMDetection: Open mmlab detection toolbox and benchmark,” *arXiv preprint arXiv:1906.07155*, 2019.

# Supplementary Material

## APPENDIX

### A. Supplementary Material Overview

*More Details about Experimental Setup (B).* Describes annotation procedures, validated GT construction, and cost breakdown used to support the main experiments.

- Annotators used microtask interfaces for bounding box drawing and activity selection, illustrated with UI screenshots (B.1).
- Validated GT was created by merging and manually deduplicating two annotation strategies, with recommendations for future designs (B.2).
- Annotation costs were derived from stable task durations using crowd workers paid hourly, ensuring fair and reproducible cost estimation (B.3).

*Further Numerical Results (C).* Presents complementary quantitative evaluations to validate the VGT and detector performance.

- Expert review of 200 images confirmed the VGT has low miss and duplicate rates, indicating high precision and recall (C.1).
- Bounding box size distribution analysis shows detectors miss smaller objects compared to the VGT (C.2).
- False positives are analyzed through qualitative examples, revealing typical error patterns in detection outputs (C.3).
- Less restrictive evaluation confirms findings across broader subsets (C.4).

*Visual Examples (D).* Provides qualitative insights into labeling ambiguity and the effectiveness of the corrected labels.

- Ambiguous cases with low agreement motivate using soft labels to capture uncertainty and improve model training (D.1).
- Visual comparisons between original and validated GT highlight missed, misaligned, and ambiguous annotations (D.2 - D.6).

### B. More Details about Experimental Setup

*1) Validated GT:* In this section, we detail the process for generating the validated ground truth (VGT), with a focus on duplicate removal during the merging of two bounding box annotation strategies.

To identify duplicates, we considered all bounding box pairs across the two strategies with an  $IoU$  greater than 0.25. Each candidate pair was manually reviewed, and boxes were marked as either duplicate or non-duplicate. The combined set of bounding boxes was created by starting with the annotations from the *Keypoint-to-Box* strategy and adding non-duplicate boxes from the *Direct Box Annotation* strategy. We chose Keypoint-to-Box as the base because these annotations were aggregated across multiple annotators and generally more precise. The keypoint-first workflow also helped annotators achieve consensus on all visible human figures before defining bounding boxes. In contrast, the Direct Box strategy resulted in

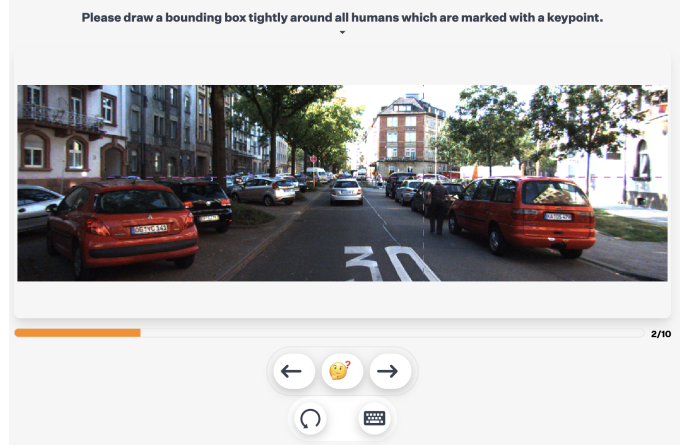


Fig. A.1: Annotator interface for microtask 1: Direct box annotation, where multiple annotators draw tight bounding boxes around all real humans not yet marked in the image.

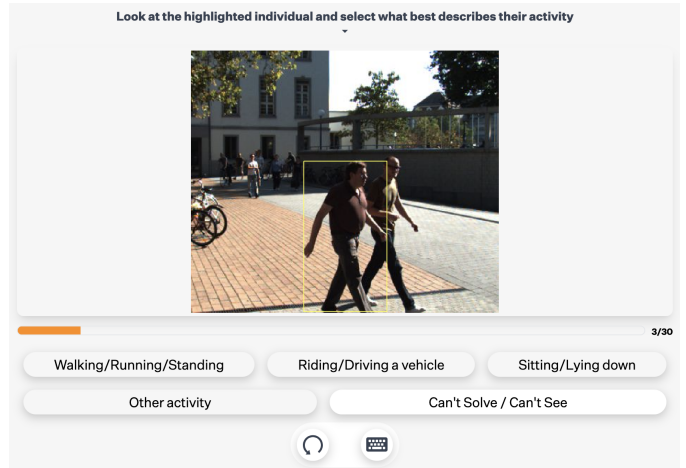


Fig. A.2: Annotator interface for microtask 6: Activity classification, where annotators select the activity of a person from predefined options: *Walking/Running/Standing*, *Riding/Driving a vehicle*, *Sitting/Lying down*, or *Other*.

frequent duplicates, often because annotators missed existing boxes or interpreted bounding boundaries differently.

Overall, we found that duplicate removal is difficult and time-consuming. In future annotation efforts, we recommend avoiding the merging of multiple annotation strategies and instead relying solely on the Keypoint-to-Box approach, with two improvements:

- 1) Increase the number of annotators in the keypoint stage and verify coverage *e.g.* by checking the false negative rate before proceeding to box drawing.
- 2) Use multiple annotators to draw bounding boxes for each identified keypoint group and add a final check to ensure no boxes were missed.

Although box aggregation generally worked well, some boxes were mistakenly merged or missing due to overlooked key-points. So we would recommend an additional round of bounding box annotation without aggregation to catch errors. Finally, we recommend including clear annotation guidelines regarding occlusion. Some annotators estimated full-body extents (including occluded regions), while others labeled only visible parts. Both are valid, but the choice should be aligned with the intended downstream task. Overall, both strategies proved highly effective for identifying all human instances, including pedestrians.

2) *Annotation Interface*: In Figure A.1 and Figure A.2 you can see examples of the used Annotation interface.

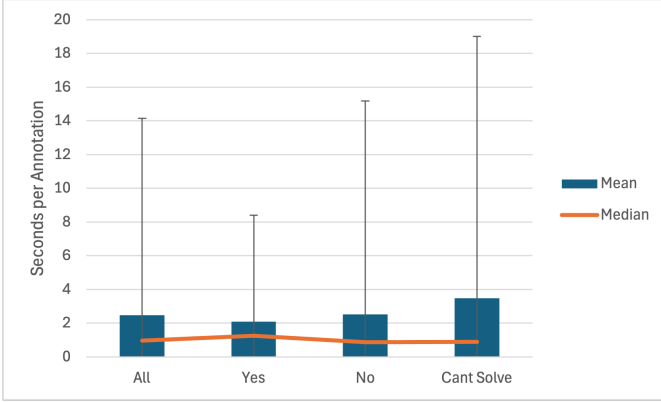


Fig. A.3: Mean, median, and variance of annotation times for microtask 4 (“Is the object in the bounding box a pedestrian?”)

3) *Costs*: We used a crowdsourced labeling provider operating in Ukraine, with a compensation rate of 4.5 € per hour per annotator. Annotation costs are calculated per bounding box correction, based on the measured annotation time for each individual label.

A detailed cost analysis is provided in the main paper, where we report the total annotation cost per corrected bounding box. A further breakdown by answer option is not necessary, as the annotation times and thus the costs do not vary significantly across answer types. This is shown in Figure A.3 for microtask 4 (“Is the object in the bounding box a pedestrian?”), where the average annotation times for the options *Yes*, *No*, and *Can’t Solve* show only minor differences. This consistency justifies the use of a unified cost estimate across all response types.

Object Detector	Accuracy	AUROC
Cascade R-CNN	94.01 ± 0.42 %	0.9107 ± 0.0010
YOLOX	95.78 ± 0.90 %	0.9892 ± 0.0051

TABLE A.1: Performance of the MetaDetect meta classification model on hold-out data, reported as mean Accuracy and AUROC with standard deviations over 5 folds.

4) *MetaDetect Performance*: Meta classification results for the MetaDetect model in terms of Accuracy and AUROC averaged over the 5 folds are listed in Table A.1.

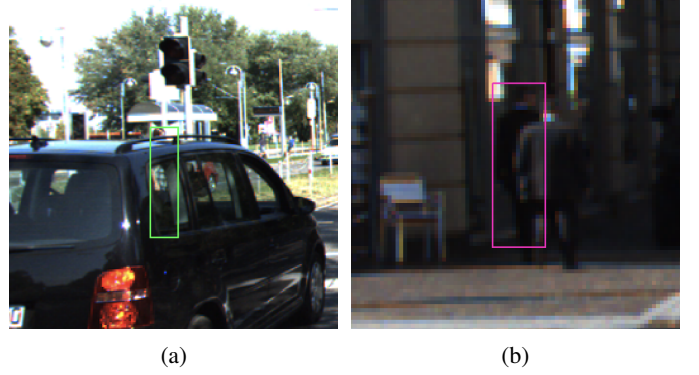


Fig. A.4: Two missing humans in the validated GT. Green box pedestrian in original data, pink bounding box found humans in Validated GT. On the left side, the human is almost completely hidden by the car and thus was most likely missed by the annotators. Since the human was detected in the original GT, we could potentially add this box by merging our boxes with the original GT. On the right side, it looks like a second person is right of the found person. In both cases the persons are extremely difficult to see.



Fig. A.5: Potential duplicate bounding boxes in the validated GT. Duplicates can occur for largely different bounding boxes e.g. for humans in cars, where one annotator annotates only the visible part of the human and another annotates the estimated shape of the human see Figure A.5a. These duplicates are not an issue for the remainder of the analysis because the probability of these bounding boxes being a pedestrian are  $< 0.5$  and thus excluded from the evaluations anyways. For one other image out of the 200 randomly, we found potentially duplicate pedestrian entries (see Figure A.5b). This scene shows a group of people in the background. Due to the resolution, it is quite difficult to see where one person ends and another begins. Based on a rating of an expert annotator, we assume that three bounding boxes (marked in orange) are actually duplicates here mainly due to imprecise bounding box drawing.

### C. Further Numerical Results

1) *Quality of Validated GT*: To verify the quality of the validated GT we needed to ensure that we did not miss (FN) or duplicated (FP) pedestrians during the annotation process. First, we manually audited 200 randomly selected VGT images by expert annotators to check if any pedestrian



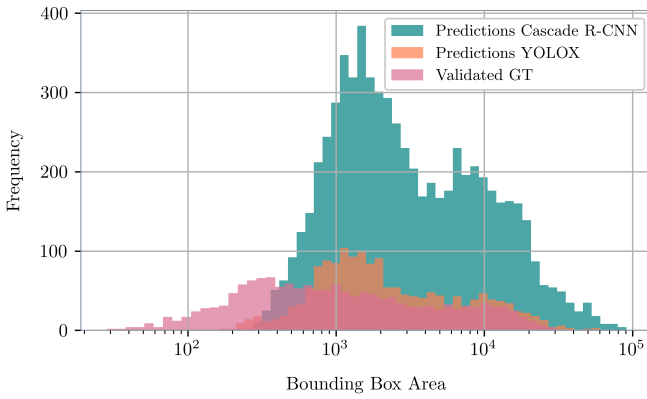


Fig. A.6: Distribution of bounding box area of validated annotations and predictions of the object detectors YOLOX and Cascade R-CNN for the class *pedestrian*.

is missing a bounding box in the dataset. We only found two examples where one could argue that a pedestrian is missing see Figure A.4. Considering that there are 377 VGT boxes with a soft label probability above 0.5 in this sample and we found only two additional pedestrians, this yields a miss rate of  $2/379 \approx 0.5\%$  and confirms the high recall of the VGT. Second, we checked if duplicate bounding boxes exist for 200 randomly selected VGT images. These are mainly introduced due to the merging of the bounding box strategies. We found one minor general issue. If the bounding boxes are too different in appearance we may not have caught them in the duplicate detection. We found potentially 3 duplicate bounding boxes with a score above 0.5 out of all bounding boxes in the sample of 200 images, see Figure A.5. This implies that  $3/377 \approx 0.8\%$  of our boxes above 0.5 are actually not pedestrians.

2) *Prediction Bounding Box Sizes*: When we analyze the size of the objects predicted by the detectors used in this study, we observe a discrepancy with the validated annotations in Figure A.6. Predictions for small objects are rare because these models did not encounter many small objects in the training data.

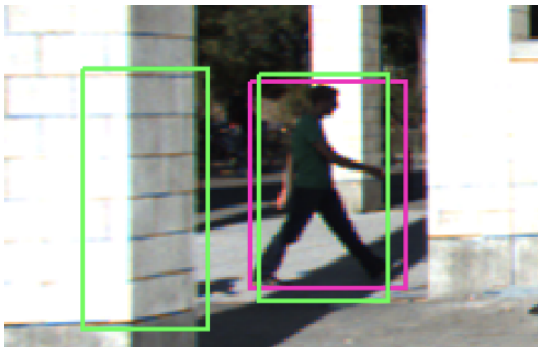


Fig. A.7: False positive detection in the KITTI dataset: A bounding box is predicted on a background region where no pedestrian is present.



Fig. A.8: False positive detection in the KITTI dataset: A bounding box is predicted on a background region where no pedestrian is present.

The primary focus of our work is identifying false negatives, *i.e.*, instances where pedestrians are present in the scene but missing from the original annotations. This task is significantly more challenging, as it requires scanning the entire image to find pedestrians that were not detected at all. In contrast, identifying false positives is comparatively easier, as it only involves verifying whether an annotated bounding box in the original ground truth actually contains a pedestrian.

Although not the central goal of this study, we still identified several 85 false positives in the original KITTI dataset based on our validated ground truth (see Figures Figure A.7 and Figure A.8). These findings suggest that our approach can also identify overlabeling errors that would otherwise remain unnoticed.

3) *Less Restrictive Analysis*: In Figure A.9 we present a less strictly filtered analysis as in the main paper. The analysis of this graph is already conducted in the main paper and thus not repeated here.

#### D. Visual Examples

1) *Analysis of Ambiguity and Uncertainty*: We analyze cases with low inter-annotator agreement, shown in Figure Figure A.10, and identify common sources of ambiguity in pedestrian detection: distant pedestrians, poor lighting conditions, and crowded scenes with occlusions. Prior work has shown that incorporating soft labels and uncertainty measures can improve model calibration, detection accuracy, and downstream performance [52], [55]. These methods are particularly effective in crowded or visually complex scenes, where binary labels fail to capture annotation uncertainty. Training with soft labels has also been shown to reduce the impact of missing ground truth labels and provide richer training signals by encoding probabilistic information.

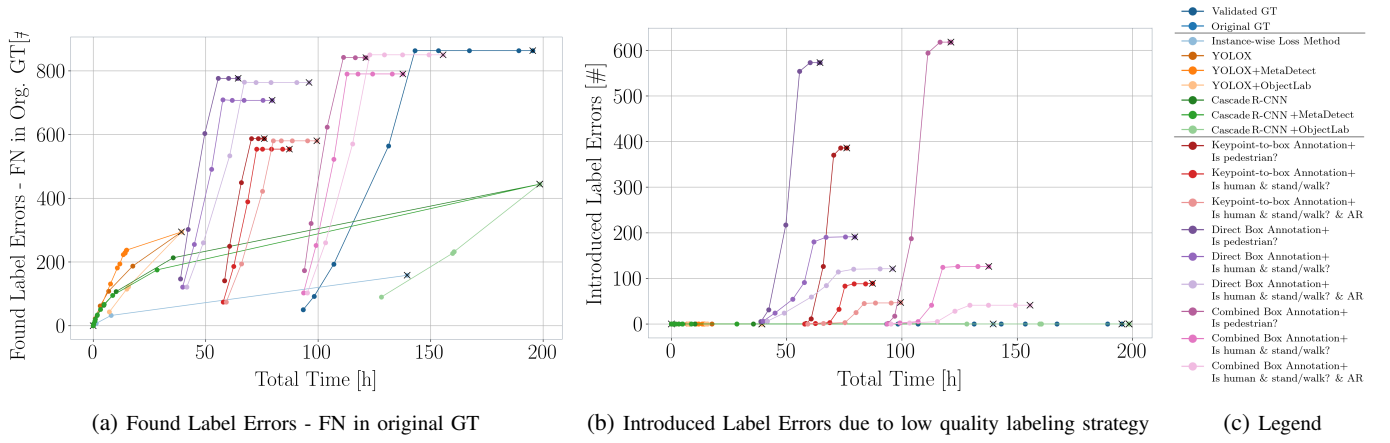


Fig. A.9: Comparison of label error detection capabilities across various methods and labeling strategies, along with their respective costs. In both figures, the x-axis represents the total annotation time, while the y-axis shows the metric of interest. Each curve corresponds to a specific method, with dots marking different model confidence thresholds. The point labeled “x” indicates the lowest threshold, corresponding to the most predictions above the threshold. As the confidence threshold increases, fewer predictions are included. Methods are grouped into three categories in the legend (c): (1) ground truth baselines (original and validated), (2) automated label error detection methods, and (3) labeling strategies combining different box annotation and semantic validation techniques. The left plot (a) shows the number of detected label errors—specifically, false negatives (FNs) in the original ground truth. The center plot (b) illustrates errors introduced by different labeling strategies, demonstrating that lower-cost strategies may lead to new annotation errors. Note that automated error detection methods assume access to validated ground truth for evaluation, but also use its high cost. For a detailed description of the evaluation metrics, refer to subsection IV-E. All boxes are pre-filtered to a minimum height of 0 pixels. A validated ground truth label is considered a pedestrian if its soft label probability exceeds 0.5. This figure is a lesser strict version of Figure 6.

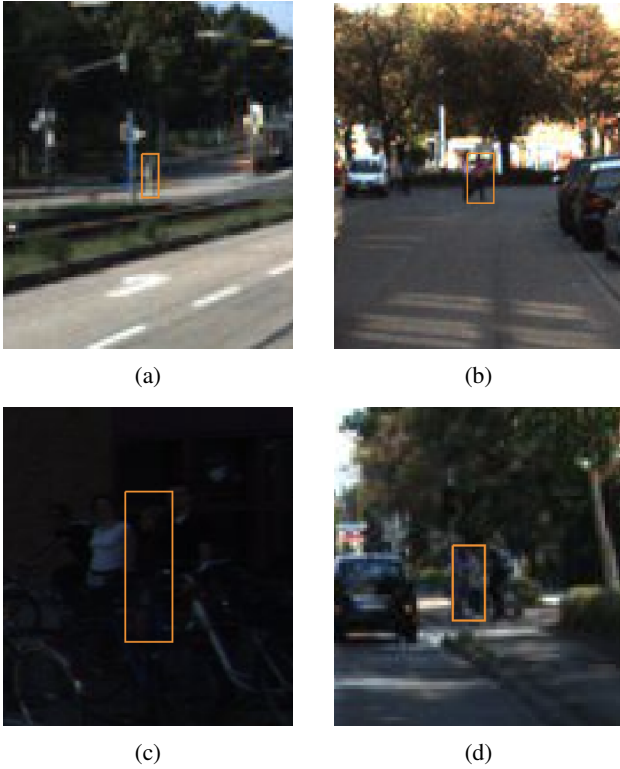


Fig. A.10: Example images with high ambiguity, where annotator disagreement is particularly pronounced.

2) *Visual Comparison of Original and Validated GT*: Here, we display examples of the label errors we identified by comparing the validated annotations with the original ones. These examples correspond to the values listed in Table 3 of the main manuscript. In the following, we consider only those label errors outside of *don't care* regions of the dataset, *i.e.*, the lower half of Table 3. First, we display all of the relatively large overlooked pedestrians and inaccurate annotations for which our validated annotations exhibit a high confidence. Then, we show random examples of other label errors, *e.g.* representing smaller objects or ambiguous cases, as distinguished in Table 3. We set a common random seed for reproducibility.

3) *Most evident overlooked objects*: In the following, we display the overlooked objects (in red color) that are not contained in original annotations (green color). These examples have a soft label probability of 0.8 or higher as well as a bounding box height of 40 pixels or more. We identified 63 such cases and order them according to the soft label probability of the validated annotations and include the original filename for verification purposes.



007265.png



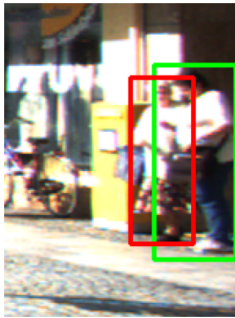
002954.png



002954.png



005367.png



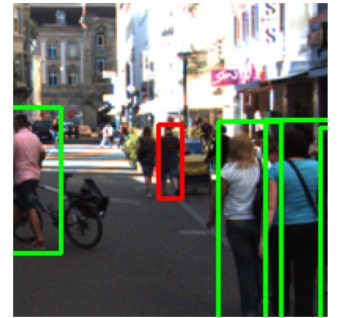
007286.png



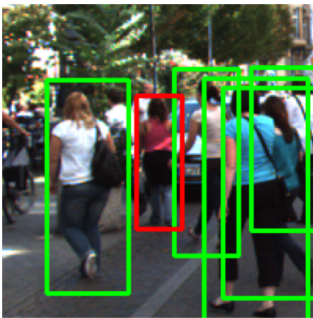
000189.png



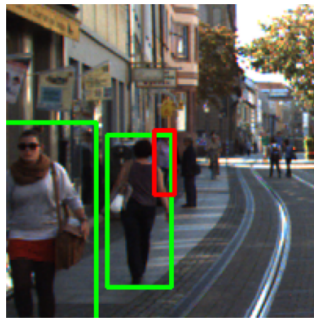
006762.png



002583.png



006427.png



003018.png



003764.png

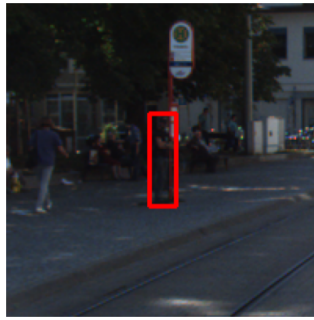


000441.png





003206.png



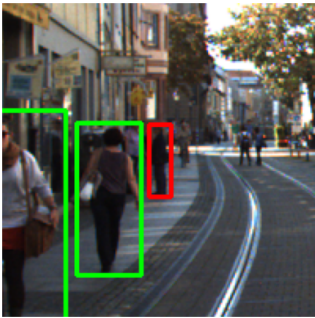
001981.png



000189.png



001786.png



003018.png



000518.png



004215.png



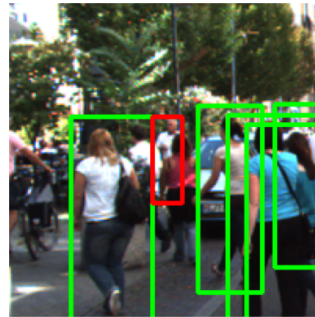
003206.png



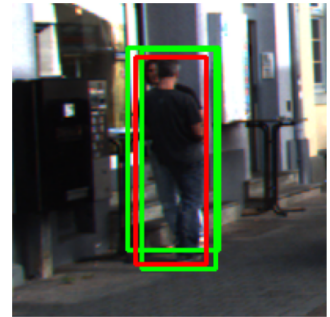
007420.png



005157.png



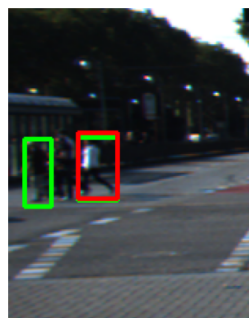
006427.png



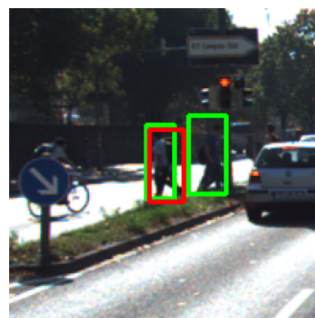
000341.png



001981.png



004215.png



004788.png

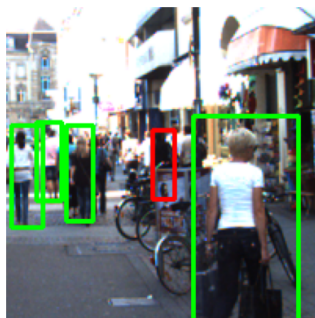


001035.png





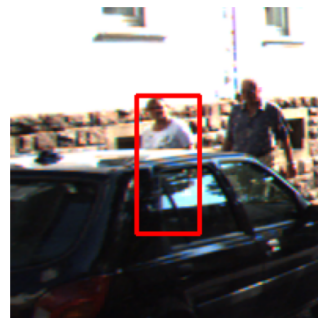
003302.png



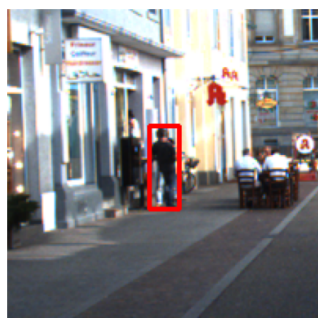
006980.png



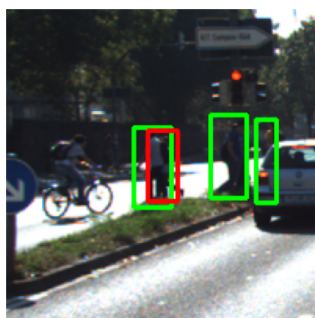
007286.png



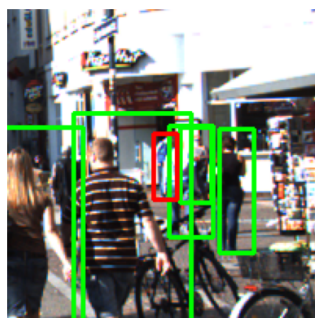
005157.png



001525.png



001640.png



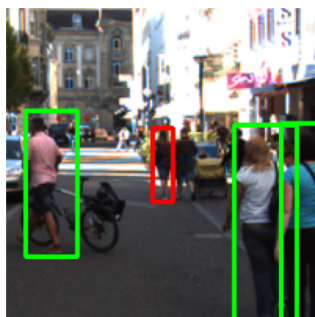
000559.png



000736.png



001372.png



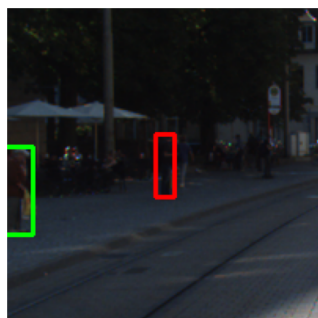
002583.png



003018.png



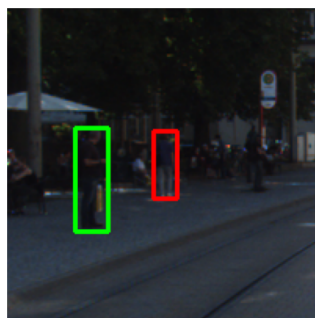
000804.png



003586.png



007161.png

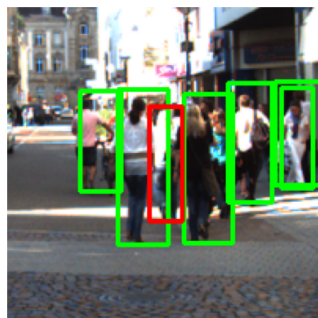


000720.png

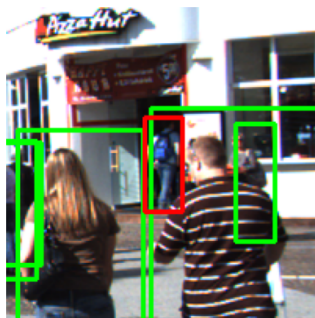


000189.png

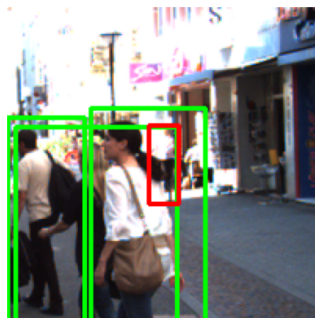




002775.png



006937.png



006427.png



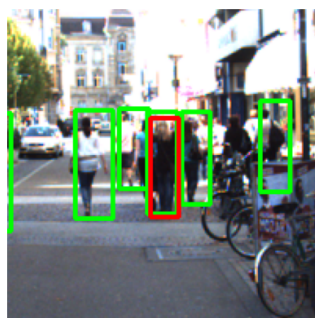
005982.png



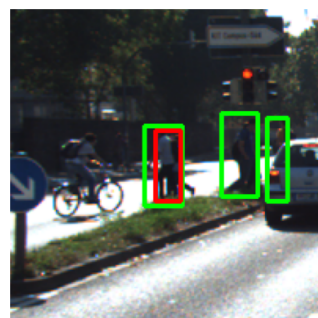
000625.png



004028.png



003718.png



001640.png



000736.png



000625.png



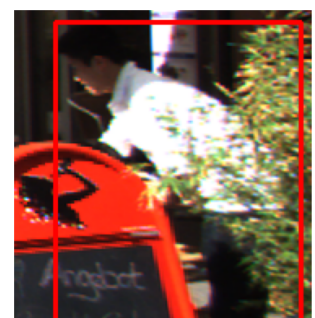
002315.png



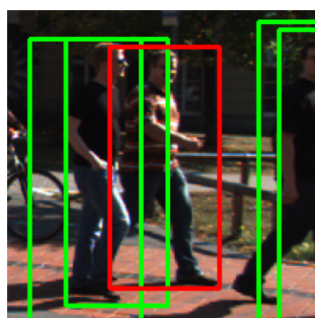
001336.png



000518.png



000496.png



001648.png



007157.png





003302.png

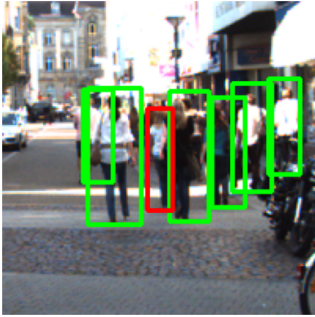


000625.png

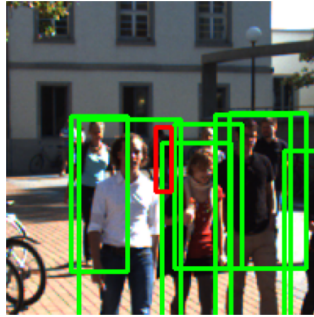


005982.png

4) *Most evident misfitting bounding boxes:* Original annotations may be inaccurate. If the original annotation does not exhibit an  $IoU$  of 0.5 with the validated one, we consider the original bounding box as misfitting. This label error is less obvious and may depend on subjectivity. We list some of the 87 mismatches we identified, sorted by the difference in  $IoU$  with the VGT. Note that many of these errors can be more interpreted as overlooked pedestrians as well but they overlap with an original bounding box annotation mainly due to duplicate GT bounding boxes.



005510.png



000966.png



005532.png



005532.png



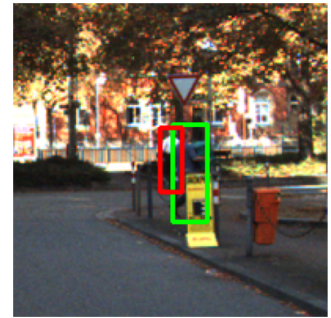
004443.png



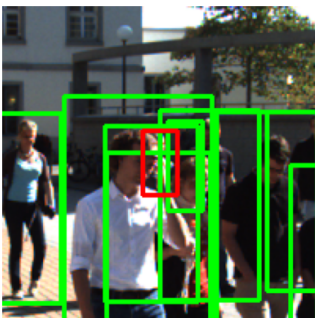
000625.png



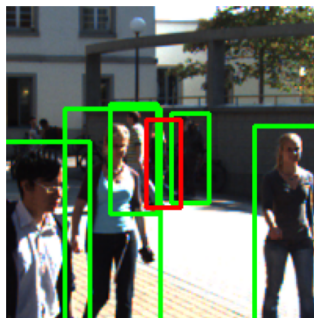
000937.png



004273.png



003502.png



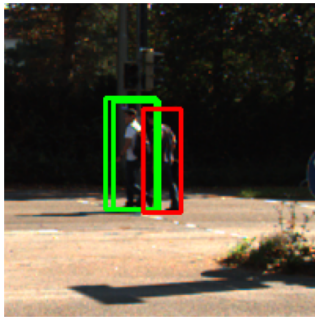
002979.png



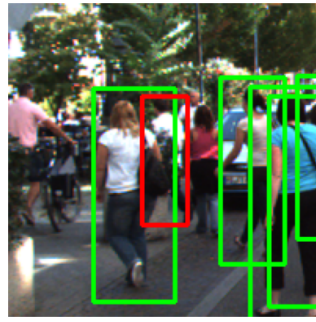
004443.png



000727.png



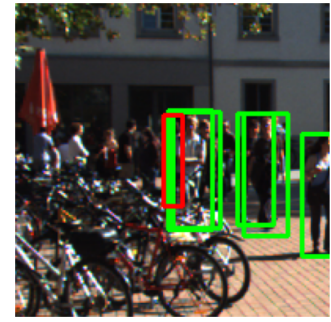
006051.png



006427.png



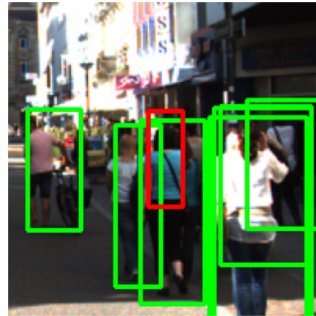
005336.png



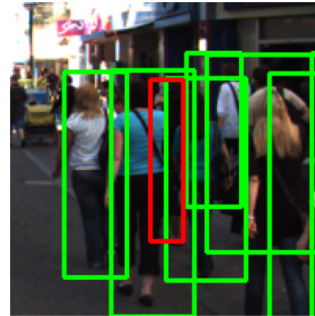
005532.png



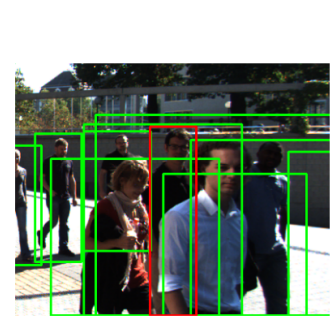
000966.png



002315.png



002583.png



002979.png

### *E. Examples of smaller but unambiguous label errors*

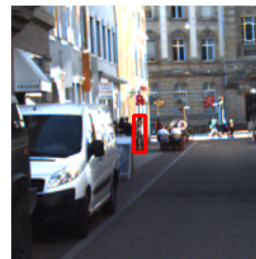
Here, we consider a random sample of overlooked pedestrians, that were assigned a soft label probability exceeding 0.8 and have a bounding box height of less than 40 pixels.



001910.png



001543.png



002699.png



003056.png



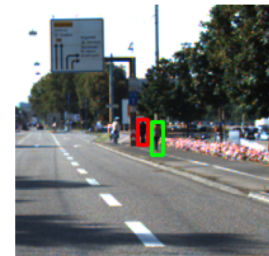
001572.png



004261.png



005433.png



005316.png





003511.png



001648.png



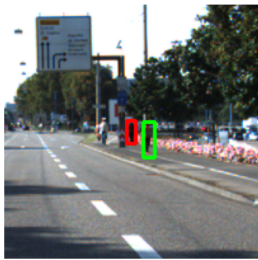
004027.png



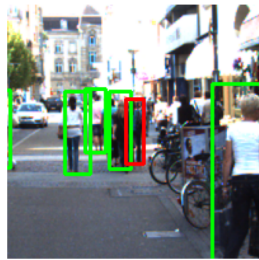
007265.png

#### F. Examples of somewhat ambiguous label errors

Here, we consider a random sample of overlooked pedestrians, that were assigned a soft label probability between 0.5 and 0.8 meaning that they represent somewhat ambiguous instances.



001424.png



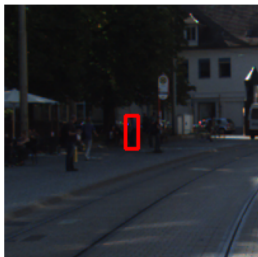
006980.png



002979.png



007118.png



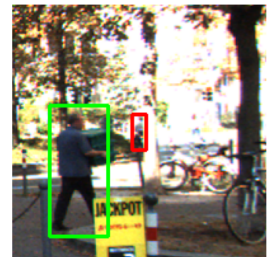
004729.png



005315.png



001543.png



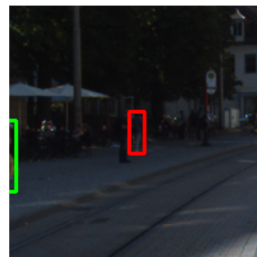
004827.png



004137.png



002979.png



003586.png



002189.png